

# On the Characterization of Nonlinear Viscoelastic Materials\*

(Received January 10, 1969)

R. A. SCHAPERY, *School of Aeronautics, Astronautics and Engineering Science  
Purdue University, West Lafayette, Indiana*

Starting with specific constitutive equations, methods of evaluating material properties from experimental data are outlined and then illustrated for some polymeric materials; these equations have been derived from thermodynamic principles, and are very similar to the Boltzmann superposition integral form of linear theory. The experimental basis for two equations under uniaxial loading and the influence of environmental factors on the properties are first examined. It is then shown that creep and recovery data can be conveniently used to evaluate properties in one equation, while two-step relaxation data serve the same purpose for the second equation. Methods of reducing data to accomplish this characterization and to determine the accuracy of the theory are illustrated using existing data on nitrocellulose film, fiber-reinforced phenolic resin, and polyisobutylene. Finally, a set of three-dimensional constitutive equations is proposed which is consistent with nonlinear behavior of some metals and plastics, and which enables all properties to be evaluated from uniaxial creep and recovery data.

The mechanical behavior of polymeric materials is described by the well-developed theory of linear viscoelasticity if stresses (or strains) are sufficiently small. This linear response range, however, is often small compared with the total range available prior to yielding or fracture (1,2,3). If a structurally efficient design is to be realized, it may, therefore, be necessary to account for nonlinear material behavior in a stress and/or deformation analysis. Of course, this does not mean linear theory loses its value for nonlinear solids as it can still serve as a useful tool in preliminary design and the study of trends.

In this paper we shall discuss certain methods of characterizing nonlinear viscoelastic solids. The total characterization process generally consists of developing stress-strain (constitutive) relations and using experimental data to evaluate the material property functions in these equations; however, we shall be primarily concerned with the latter phase, starting with explicit relations between stress and strain history. Examples are given utilizing only polymer data; but, as we have shown elsewhere (4), the constitutive theory used here appears to have wide applicability in that it includes mechanical behavior observed for such different materials as met-

als, soils, and biological tissue. These examples will serve to illustrate methods of data reduction and show how the theory provides guidelines for designing experimental programs.

Very general constitutive theories have been developed for relating stress and strain histories (5). For practical reasons, however, the stress-strain equations one actually uses in characterizing a given material must be the result of considerable simplification. Furthermore, the material property functions contained in these equations are usually evaluated using data from specimens under stress states (e.g., uniaxial tension, tension plus torsion, etc.) and histories (e.g., constant stress, constant strain, etc.) which are simpler than those existing in actual service conditions.

Because of these factors, a well-designed experimental program should be one that provides data beyond that needed to evaluate property functions. Additional experimental results should be obtained for making critical checks on the accuracy of the theory in predicting behavior under loading as close as practicable to that in the anticipated structural application. These checks may range from tests of specimens under uniaxial stress histories which are more complex than those used in evaluating properties to studies of models and prototypes. The strength and complexity of nonlinearities, as well as

\* Presented at the SPE Symposium on Design of Experiments and Data Analysis in Plastics Engineering, September 1968.

the amount of experience one has acquired with a given material, obviously dictate the extent of experimental verification that should be made.

Stress-strain relations in the form of a sum of multiple integrals appear to have received the most attention in recent years for characterizing polymeric materials. This type of representation was developed by Green and Rivlin (6) and Green, Rivlin, and Spencer (7), and has been applied by several investigators (Ref. 8 to 11). It is very appealing theoretically since it is not limited to a particular material or class of materials, and permits one to construct approximations with respect to any order of nonlinearity desired. However, the multiple integral representation becomes impractical with strong nonlinearities, unless one assumes the kernels can be written in terms of products of a single function (8, 11), and it does not take advantage of certain simplicity that exists in the mechanical behavior of many polymers and non-polymers.

Concerning this latter point, it is found that time- or frequency-dependence of mechanical response in the nonlinear range can normally be expressed in terms of linear viscoelastic properties. This is especially apparent in strain response to constant stress (creep test) and stress response to constant strain (relaxation test).

This simplicity in mechanical behavior has served to motivate the development of single-integral constitutive equations from thermodynamic principles (4, 12, 13). They are easily applied, as we shall demonstrate in this paper, since they have a form which is very similar to the Boltzmann superposition integral used in linear viscoelastic theory. Moreover, experimental demands are reduced because the only time-dependent properties needed are those which exist in the linear viscoelastic range. We should add that these stress-strain equations represent a generalization of a modified superposition theory proposed by Leaderman several years ago (14).

In the next section, the stress-strain equations are given for uniaxial loading. It is shown that they contain, as special cases, the type of nonlinear behavior which is commonly observed in creep and relaxation tests. The discussion in this and subsequent sections is primarily concerned with characterization of nonaging solids under fixed environmental conditions; however, in certain important cases the effect of temperature and humidity changes, and even aging, can be taken into account by means of minor analytical extensions, and these are indicated at the conclusion of this second section.

Some methods of evaluating material properties and checking the accuracy of the theory are then given in the third section. They are illustrated using creep and recovery data on nitrocellulose film and glass fiber-reinforced phenolic resin, and stress relaxation data on polyisobutylene (PIB).

Finally, multiaxial stress-strain equations are given in the fourth section. As an illustrative example, creep data obtained under combined tension and tor-

sion are used to characterize polyvinylchloride (PVC). We show that nonlinear properties can be expressed (approximately) in terms of the octahedral shear stress.

## CONSTITUTIVE EQUATIONS FOR UNIAXIAL LOADING

This and the next section deal with characterization of a specimen under a uniform, uniaxial stress  $\sigma = \sigma(t)$  and strain  $\epsilon = \epsilon(t)$ . By definition,  $\sigma$  is axial force divided by cross-sectional area in the unstrained state and  $\epsilon$  is change in length divided by unstrained length; these definitions are used here regardless of strain magnitude. This choice of stress and strain satisfies the condition that  $\sigma d\epsilon$  must be equal to an increment of work per unit initial volume, according to the underlying thermodynamic theory (12, 13). It should also be realized that by simply changing notation we can apply all uniaxial theory to other stress and strain pairs which satisfy the virtual work condition; simple shear stress and strain is one such pair.

For reference purposes, we shall first record some relations describing linear viscoelastic behavior of a nonaging specimen under fixed environmental conditions.

### Linear Equations

When a constant stress is applied at  $t = 0$ , the ratio of strain response to stress input is a function only of time; viz.,

$$\frac{\epsilon}{\sigma} = D(t) \quad (1)$$

where  $D(t)$  is the so-called creep compliance. The stress-strain relation for this "creep test" can be put in the equivalent form:

$$\epsilon = D_o \sigma + \Delta D(t) \sigma \quad (2)$$

where

$$D_o \equiv D(0) = \text{initial value of compliance}$$

and

$$\begin{aligned} \Delta D(t) &\equiv D(t) - D_o \\ &= \text{transient component of compliance} \end{aligned}$$

Similarly, application of a constant strain at  $t = 0$  (relaxation test) provides the stress relaxation modulus  $E(t)$ :

$$\frac{\sigma}{\epsilon} = E(t) \quad (3)$$

or, equivalently,

$$\sigma = E_e \epsilon + \Delta E(t) \epsilon \quad (4)$$

where

$$E_e \equiv E(\infty) =$$

equilibrium or final value of modulus

$$\Delta E(t) \equiv E(t) - E_e =$$

transient component of modulus

When  $D(t)$  is known, we can calculate the strain response to an arbitrary stress input by means of the Boltzmann superposition integral<sup>2</sup>,

$$\epsilon = D_o \sigma + \int_{0-}^t \Delta D(t - \tau) \frac{d\sigma}{d\tau} d\tau \quad (5)$$

Creep Eq. 2 is recovered from Eq. 5 by substituting  $\sigma = \sigma' H(\tau)$  into Eq. 5, where  $\sigma'$  is constant, and

$$H(\tau) \equiv \begin{cases} 0, \tau < 0 \\ 1, \tau > 0 \end{cases} \quad (6)$$

and then dropping the prime.

Relaxation data can be used in a similar way to calculate stress response to an arbitrary strain input:

$$\sigma = E_e \epsilon + \int_{0-}^t \Delta E(t - \tau) \frac{d\epsilon}{d\tau} d\tau \quad (7)$$

It is important to recognize that linear stress-strain behavior of a given material is defined completely by either Eq. 5 or 7. This implies  $E(t)$  can be calculated from  $D(t)$ , or vice versa; methods for making such calculations are described in (1, 15). Since the evaluation of either material property function from experimental data is accomplished very simply using Eq. 1 or 3, experimental factors alone determine which is the more desirable test. As we shall see, this conclusion is not necessarily true for nonlinear materials because of additional material properties that enter.

### Nonlinear Equations

Turning now to nonlinear constitutive equations, we observe that the thermodynamic theory developed in (12, 13) permits us to express material properties in terms of either stress or strain. When stress is treated as an independent state variable, the author's theory in (13) yields the following equation:

$$\epsilon = g_o D_o \sigma + g_1 \int_{0-}^t \Delta D(\psi - \psi') \frac{dg_2 \sigma}{d\tau} d\tau \quad (8)$$

where  $D_o$  and  $\Delta D(\psi)$  are the previously defined components of the linear viscoelastic creep compliance,  $\psi$  is the so-called reduced-time defined by

$$\psi \equiv \int_0^t dt' / a_\sigma[\sigma(t')] \quad (a_\sigma > 0) \quad (9a)$$

and

$$\psi' \equiv \psi(\tau) \equiv \int_0^\tau dt' / a_\sigma[\sigma(t')] \quad (9b)$$

and the material properties  $g_o$ ,  $g_1$ ,  $g_2$ , and  $a_\sigma$  are functions of stress. By comparing (5) and (8), we see that  $g_o = g_1 = g_2 = a_\sigma = 1$  when the stress is sufficiently small. Furthermore, these stress-dependent properties have specific thermodynamic significance; changes in  $g_o$ ,  $g_1$ , and  $g_2$  reflect third and higher order

dependence of the Gibb's free energy on the applied stress, and  $a_\sigma$  arises from similar high-order effects in both entropy production and free energy.

A constitutive equation with strain-dependent properties is given by the theory in (12), wherein strain, rather than stress, is used as an independent state variable. It can be put in the same form as Eq. 8; viz.,

$$\sigma = h_e E_e \epsilon + h_1 \int_{0-}^t \Delta E(\rho - \rho') \frac{dh_2 \epsilon}{d\tau} d\tau \quad (10)$$

with the reduced-time,  $\rho$ , defined as

$$\rho \equiv \int_0^t dt' / a_\epsilon[\epsilon(t')] \quad (a_\epsilon > 0) \quad (11a)$$

and

$$\rho' \equiv \rho(\tau) = \int_0^\tau dt' / a_\epsilon[\epsilon(t')] \quad (11b)$$

The strain-dependent properties are  $h_e$ ,  $h_1$ ,  $h_2$ , and  $a_\epsilon$ ; variations in the first three are due to third and higher order strain effects in the Helmholtz free energy, while changes in property  $a_\epsilon$  arise from similar strong strain influences in both entropy production and free energy.

It should be pointed out that notation in Eq. 10 has been changed somewhat from that in (12) for convenience in applications and to bring out the similarity between the two constitutive equations.

As a means of illustrating the type of behavior described by these equations and of providing a preliminary indication of their validity for different materials, we shall examine the form they assume for creep (constant stress) and relaxation (constant strain) tests.

### Creep and Relaxation Behavior

Substituting a constant stress,  $\sigma$ , into Eq. 8, and recognizing that  $dg_2 \sigma / d\tau$  is zero except at  $\tau = 0$ , yields

$$\int_{0-}^t \Delta D(\psi - \psi') \frac{dg_2 \sigma}{d\tau} d\tau = \Delta D(\psi) \times \int_{0-}^t \frac{dg_2 \sigma}{d\tau} d\tau = \Delta D\left(\frac{t}{a_\sigma}\right) g_2 \sigma \quad (12)$$

where definition (Eq. 9) has also been used. Thus, the nonlinear creep compliance,  $D_n$ , is

$$D_n \equiv \frac{\epsilon}{\sigma} = g_o D_o + g_1 g_2 \Delta D\left(\frac{t}{a_\sigma}\right) \quad (13)$$

When a constant strain,  $\epsilon$ , is substituted into Eq. 10, a similar relation is derived for the nonlinear relaxation modulus,  $E_n$ :

$$E_n \equiv \frac{\sigma}{\epsilon} = h_e E_e + h_1 h_2 \Delta E\left(\frac{t}{a_\epsilon}\right) \quad (14)$$

There is a considerable amount of published creep and relaxation data on a variety of materials which fit the special cases expressed in Eq. 13 and 14.

\* Without loss in generality, we assume the material is unloaded for all  $t < 0$ . If a discontinuity in  $\sigma(t)$  occurs at the origin, it must be included in the range of integration; accordingly, the lower limit,  $0-$ , is defined as  $\tau = 0 - |\gamma|$  with  $\gamma \rightarrow 0$ .

Leaderman (14) found that the creep compliance of mechanically conditioned textile fibers can be described by an equation that is equivalent to Eq. 13 with  $g_o = a_\sigma = 1$ ; viz.,

$$D_n = D_o + g_1 g_2 \Delta D(t) \quad (15)$$

Other equations for creep strain,  $\epsilon = D_n \sigma$ , of metals and polymers are summarized by Thorkildsen (3). Of particular interest in this summary is the expression reported by Findley and co-workers on many monolithic and composite polymeric materials. We obtain their expression from Eq. 13 by setting

$$g_o = \frac{\sinh \sigma/\sigma_e}{\sigma/\sigma_e} \quad (16a)$$

$$\frac{g_1 g_2}{a_\sigma^n} = \frac{\sinh \sigma/\sigma_m}{\sigma/\sigma_m} \quad (16b)$$

and

$$\Delta D(\psi) = D_1 \psi^n \quad (16c)$$

Hence,

$$D_n = \frac{\sinh \sigma/\sigma_e}{\sigma/\sigma_e} D_o + \frac{\sinh \sigma/\sigma_m}{\sigma/\sigma_m} D_1 t^n \quad (16d)$$

where the constants  $\sigma_e$ ,  $\sigma_m$ ,  $D_1$ , and  $n$  have values that depend on the particular material. It is quite common that the initial elastic response is practically linear even though the creep is strongly nonlinear; i.e.,  $\sigma_e \gg \sigma_m$ . Also, the usual range for the exponent is  $0 < n < 0.5$ . It is to be noted that the stress-dependence of creep rate,  $\dot{\epsilon} = \dot{D}_n \sigma$ , determined by Eq. 16d, is consistent with a simple molecular model based on Eyring's rate process theory; this model is reviewed in (3). The same model has been used to explain the creep rate observed for clay soils (16), which is also described by Eq. 16d.

It must be emphasized that we do not intend to limit  $\Delta D(\psi)$  in this paper to the power law (Eq. 16c). Indeed, a graphical method will be proposed for determining nonlinear properties, one that does not require analytical functions for either  $\Delta D(\psi)$  or  $\Delta E(\rho)$ . However, we want to call attention to the fact that thermodynamic theory (13), molecular models (1), and the familiar Kelvin model, consisting of springs and dashpots (15), provide the representation

$$\Delta D(\psi) = \sum_{r=1}^N D_r (1 - e^{-\psi/\tau_r}) + D_s \psi \quad (17)$$

where  $D_r$ ,  $D_s$ , and  $\tau_r$  are positive constants;  $\tau_r$  is called a "retardation time." The term  $D_s \psi$  is the so-called steady-flow component, and leads to nonrecoverable or residual strain following removal of the stress; the coefficient  $D_s$  is often negligible, except for uncrosslinked amorphous polymers above their glass-transition temperature. Now, it is well known that power-law (Eq. 16c) can be derived from series (Eq. 17); specifically, we set  $D_s = 0$ , approximate the series by an integral over a continuous distribution of retardation times, and use a power law for the resulting retardation spectrum (15).

Some of the creep expressions in (3) exhibit a steady-flow component which is not contained in the present theory unless  $D_s$  is made a function of stress. Such behavior is actually allowed by the thermodynamic theory (13), but in this paper we shall, for simplicity, assume  $D_s$  is constant. Since the steady-flow component of strain in polymers arises physically from large relative motion between molecules, rather than from the limited molecular motion that produces the exponential series in Eq. 17, it should not be surprising to find different nonlinearities in these two types of flow. However, based on a study made by Findley and Peterson (17), the nonlinear steady-flow term reported by some investigators may be artificial, owing to the particular curve-fitting method employed.

Considering nonlinear relaxation behavior now, we first observe that most available data are on soft materials. The lack of relaxation data on hard materials is, of course, due to the experimental problem of maintaining a constant deformation with a relatively flexible loading device.

Small strain behavior of textile fibers often obeys the relation (18, 19),

$$E_n = E_e + \Delta E(t/a_e) = E(t/a_e) \quad (18)$$

which follows from Eq. 14 when  $h_e = h_1 h_2 = 1$ . The strain, therefore, simply changes the intrinsic time scale. The molecular origin of this behavior is not clear; but it is found that a small increase in strain accelerates the relaxation process, which suggests the free volume interpretation may be applicable since Poisson's ratio is less than one-half (1, p. 352).

In contrast, the effect of large strain on relaxation of unfilled polymers in their rubbery state seems to be described quite well by letting  $h_e = h_1 h_2$  and  $a_e = 1$  (20, 21); viz.,

$$E_n = h_1 h_2 E(t) \quad (19)$$

This product form has also been found for filled polymers under small strains (22); however, the more general representation (Eq. 14) may be needed in the presence of filler-particle interactions and separation between filler and matrix (23).

Although we have shown that behavior observed for a variety of materials is consistent with Eq. 13 or 14, there is no basic reason to expect that a given material will agree with *both* representations unless, of course, it is approximately elastic (i.e.,  $\Delta D \simeq \Delta E \simeq 0$ ) or linearly viscoelastic.

To expand upon this point, the relaxation modulus predicted by Eq. 8 will be compared with Eq. 14 for a special case. First, we invert Eq. 8 by recognizing that it can be reduced to a linear viscoelastic equation connecting an input  $g$ , say, and response,  $h$ , if the integration variable is changed to reduced time  $\psi'$  (using  $d\tau = a_\sigma d\psi'$ ), the input,  $g$ , is defined as

$$g \equiv g_2 \sigma \quad (20a)$$

and the response,  $h$ , is given by

$$h \equiv \frac{\epsilon}{g_1} + \left( g_2 - \frac{g_0}{g_1} \right) D_0 \sigma \quad (20b)$$

Thus, the inverse of Eq. 8 is

$$g = E_e h + \int_{0-}^t \Delta E(\psi - \psi') \frac{dh}{d\tau} d\tau \quad (21)$$

which is clearly not equivalent to Eq. 10 in this general form, and does not generally reduce to an algebraic relation, such as Eq. 14, when the strain is constant. On the other hand, for a material in which  $g_1 = a_\sigma = 1$  and  $D_0 = 0$ , Eq. 21 yields the nonlinear relaxation modulus,

$$E_n = E(t)/g_2(\sigma) \quad (22)$$

corresponding to the creep compliance

$$D_n = g_2(\sigma) D(t) \quad (23)$$

For arbitrary properties  $E(t)$  and  $g_2(\sigma)$ , (22) is not contained in Eq. 14; but if we further assume the familiar power law for high stresses,  $g_2 \simeq C_2 \sigma^m$ , and the creep compliance,  $D \simeq D_1 t^n$  (where  $C_2$ ,  $D_1$ ,  $n$ , and  $m$  are constants), we finally obtain a relaxation modulus that is a special form of Eq. 14:

$$E_n = \left( \frac{\sin n\pi}{n\pi D_1 C_2} \right) \frac{1}{1+m} \frac{1}{(t)} - \frac{n}{1+m} \frac{1}{(\epsilon)} \quad (24)$$

where the exact relation  $D(t)E(t) = \sin n\pi/n\pi$  (1, p. 71) has been used. The assumption of a power law for  $a_\sigma$ , as well as  $g_2$ , leads to the same form of relaxation modulus but with different exponents.

It is seen that modulus Eq. 24 can be written either as Eq. 18 or 19. Because this result is based on the use of power laws for nonlinearity and time-dependence, which are often valid approximations, at least over a limited range, the nonlinear response of a particular material may indeed be consistent with both Eq. 13 and 14, as reported in (2). Clearly, this consistency does not mean one is free to use either constitutive Eq. 8 or 10 for predicting response under all other loading histories. However, it is noticed that there are three nonlinear functions available for fitting data; hence, both equations may be acceptable characterizations if nonlinearity is weak, or if the properties are determined from specimens subjected to loading which is not too different from that expected in the structural application of interest.

The question of which of the two constitutive Eq. 8 and 10 is the fundamentally more appropriate one for a given material may, in some cases, be academic in view of the preceding comment. In general, however, it would be highly desirable to have more of a physical basis than now exists for choosing one in preference to the other. Molecular interpretations of nonlinear behavior were referenced above, but they are too limited to discriminate between the various sources of nonlinearity in free energy and entropy production, as reflected by the several nonlinear property functions in Eq. 8 and 10.

We further observe that the underlying thermodynamic theory restricts Eq. 8 to small strains,\* but experimental information is needed to define "small" quantitatively. Certainly this equation cannot be expected to apply when structural changes, and consequent nonlinearity, occur that are closely related to strain level; possible examples are orientation of drawn fibers and formation of vacuoles in filled systems. In contrast, Eq. 10 is not restricted to small strains, although its ability to reflect structural changes is not yet known.

Consequently, the current state is such that one must rely almost entirely on experimental information for determining the range of validity of constitutive Eq. 8 and 10, and for the evaluation of the nonlinear material properties.

### Modified Superposition Principles

The simple product form of nonlinear creep compliances (Eq. 15 and 16d) and relaxation modulus (Eq. 19) has motivated the use of constitutive equations which are slightly modified versions of the Boltzmann integral representation in linear theory. Leaderman (14) proposed and applied a so-called modified superposition principle (MSP) which we can derive from Eq. 8 by setting  $g_0 = g_1 = a_\sigma = 1$ ; specifically,

$$\epsilon = D_0 \sigma + \int_{0-}^t \Delta D(t - \tau) \frac{dg_2 \sigma}{d\tau} d\tau \quad (25)$$

A similar inverse form, corresponding to the special case of Eq. 10 for which  $h_e = h_2$  and  $h_1 = a_\epsilon = 1$ , has also been suggested (20, p. 139; 21).

More recently, Findley and Lai (24) used an MSP to predict strain response of unplasticized PVC to discontinuously applied tensile and shearing stresses. Under tensile (or shearing) stress alone, their theory is a special case of Eq. 8 for materials whose creep compliance is contained in representation (Eq. 13). Namely, we obtain their MSP by assuming  $g_1 = a_\sigma = 1$  and then evaluating the integral in Eq. 8 for a stress which is applied stepwise in time; application of the MSP in (24) is limited to this case, together with the power law (Eq. 16c). It should be added that a closely related superposition technique is given in (25); but it is not exact for even the limiting case of a nonlinear elastic material, and consequently cannot be expected to be as accurate as the more recent one in (24).

Pipkin and Rogers (26) proposed a multiple-integral series representation for stress-strain behavior, with Findley and Lai's MSP appearing as the first term in the series. Equations for stress (and strain) varying continuously and/or stepwise are given in (26), along with applications to unplasticized PVC and a polyurethane foam; nonlinear creep compliances of these materials are special cases of Eq. 13.

A review of the referenced papers shows that the modified superposition principles have met with

\* A possible extension of Eq. 8 for large strains is given in Ref. 13.

varying degrees of success, their accuracy depending on the particular material as well as on the type of loading. Since they are strictly empirical generalizations of a linear stress-strain equation, such results are not surprising. On the other hand, constitutive Eq. 8 and 10 are expected to be more successful, as we will illustrate later for the wide range of materials having compliance (Eq. 13) or modulus (Eq. 14); this follows, of course, from the presence of additional nonlinear properties as well as the thermodynamic basis for these more general equations.

### Generalizations

There are certain analytical generalizations of Eq. 8 and 10 that are easily made, and can serve to extend their range of applicability. First, we recall that  $a_\sigma$  and  $a_\epsilon$  are assumed above to depend only on stress or strain, respectively. However, the only thermodynamic restriction is that these coefficients be positive for stable materials (4, 13). Additional variables may therefore enter, depending on the material, loading, and environment.

Concerning additional mechanical variables that could be needed in the functions,  $a_\sigma$  and  $a_\epsilon$ , we observe that if strain rate or stress rate is included, we obtain the rate-independent plasticity theory of metals as a special case (4, 13). Moreover, the so-called mechanical equation of state and strain hardening theories (3, 25) (which have been successfully applied to metals and plastics under *non-decreasing* loads) are derived from Eq. 8 (or 10) by assuming  $a_\sigma$  (or  $a_\epsilon$ ) depends on both stress and strain, and  $\Delta D(\psi)$  is that for a Maxwell model (3); i.e.,  $\Delta D \equiv D_s \psi$ . Of course, the need for both stress and strain in  $a_\sigma$  (or  $a_\epsilon$ ) may have been artificially created by using an overly simplified creep compliance.

Turning now to environmental factors, let us consider first the effect of a spatially uniform temperature on the mechanical behavior of a specimen. It is well known that the dominant effect of temperature on amorphous polymers over relatively broad temperature ranges is to shift the intrinsic time-scale (2, 20, 27); materials that have such temperature-dependence are often called "thermorheologically simple" (20). The same phenomenon is observed with semicrystalline and crystalline materials, including metals (28), as long as structural changes (such as a change in the degree of crystallinity) do not occur.

The present theory may be extended to include this behavior by introducing temperature as an argument of the coefficients  $a_\sigma$  and  $a_\epsilon$ ; viz.,

$$a_\sigma = a_\sigma(\sigma, T), a_\epsilon = a_\epsilon(\epsilon, T) \quad (26)$$

In the presence of a transient temperature, due account of this must be taken when calculating reduced-times by means of the integrals (Eq. 9 and 11); observe that  $a_\sigma(0, T)$  and  $a_\epsilon(0, T)$  are not unity, except at some reference temperature.

Thermorheologically simple behavior can be interpreted in terms of the thermodynamic theory in (12,

13). Specifically, it results for materials having a free energy function that depends, at most, on temperature change to the second order, and an entropy production that is strongly temperature-dependent through a scalar factor. If the free energy is strongly affected by temperature (as it would be when structural changes occur or the dominant molecular modes of motion change), the thermodynamic theory (12, 13) shows that constitutive relations (Eq. 8 and 10) may still be valid with constant or transient temperatures; however, all or some of the functions,  $g_0$ ,  $g_1$ ,  $g_2$ ,  $h_e$ , and  $h_1$ , but not  $h_2$ , would depend on temperature.

There is some experimental evidence available on semicrystalline polymers that supports this generalization. In particular, let us consider its implication for linear viscoelastic behavior, as described by Eq. 10. For this case  $h_2 = 1$ , but  $h_e$  and  $h_1$  may vary with temperature; if  $h_e = h_1$ , Eq. 10 reduces to

$$\sigma = h_e \int_{0-\epsilon}^t E(\rho - \rho') \frac{d\epsilon}{d\tau} d\tau \quad (27)$$

The relaxation modulus at an arbitrary temperature then becomes

$$E(t, T) \equiv \frac{\sigma}{\epsilon} = h_e(T) E\left(\frac{t}{a_T}\right) \quad (28)$$

where  $a_\epsilon = a_\epsilon(0, T) \equiv a_T(T)$ . Now if a material satisfies Eq. 28, curves of  $\log E(t, T)$  vs  $\log t$ , for different temperatures, can be shifted rigidly along the two axes to form a "master curve"; this master curve is defined as the relaxation modulus for some arbitrarily chosen reference temperature, and the amount of vertical and horizontal shifting provides values of the so-called "shift factors"  $h_e$  and  $a_T$ . The real part of the complex modulus, as calculated from Eq. 27, will exhibit the same behavior. This modulus for a semicrystalline polymer, polyethylene, is shown in (29) to conform to this reduction scheme; it is suggested that the horizontal shift factor,  $a_T$ , primarily reflects temperature-dependence of the amorphous regions, while the horizontal shift factor accounts for the change in rigidity of the crystalline regions.

Attention is called to the fact that this constant temperature behavior is not sufficient proof of the validity of Eq. 27; additional tests are needed to verify this equation in the presence of time-dependent temperatures. The author is not aware of any publication that covers such tests on either amorphous or crystalline polymers, even in their linear viscoelastic range of behavior.

In order to apply the constitutive equations in this paper to transient temperature conditions, it is necessary to use a strain defined in terms of specimen length at some reference temperature,  $T_R$ , say. It is often permissible to assume thermal expansion of linear viscoelastic materials as a unique function of temperature. If one finds this to be true for the nonlinear case, the strain in Eq. 8 and 10 can be replaced by  $\epsilon_0 - \Delta T$ , where  $\epsilon_0$  is total strain

measured from temperature  $T_R$ , and  $\Delta_T = \Delta_T(T)$  is the thermal expansion. On the other hand, thermal expansion could depend on temperature history and strain level as well, especially near the glass-transition temperature of amorphous polymers or with phase changes. Ref. 12 and 13 should be consulted in order to account for such behavior.

Moisture is another important environmental parameter that affects the mechanical behavior of some polymers (27, 30), in that it may have an appreciable influence on the time-scale factor,  $a_t$  or  $a_\sigma$ . Accompanying absorption of water is an expansion that should be added to the thermal expansion indicated above.

Changes in the time-scale factor for polymers may be due to changes in free volume. Ferry and Stratton (31) use this concept to derive equations for the dependence of  $a_t$  on temperature, confining pressure, strain, and moisture or other plasticizer concentration.

So far, we have suggested generalizations of constitutive Eq. 8 and 10 that account for parameters which can be externally controlled. However, aging phenomena due to slow chemical changes could also exist. The form of Eq. 8 and 10 may still be applicable in this case, but all or some of the properties will depend explicitly on aging time. If the time scale for appreciable aging is long compared to the time over which a load is applied, characterization methods obviously will be the same as for a nonaging material.

On the other hand, when these two time scales are comparable, experimental demands, especially, are greatly increased. For example, consider the problem of characterizing a linear viscoelastic material for isothermal applications. With sufficiently small stresses, we can write

$$\epsilon = \int_{0-}^t D(t-\tau, \tau) \frac{d\sigma}{d\tau} d\tau \quad (29)$$

where  $t = 0$  at the start of the aging process. (This equation is simply a statement of the superposition property of an arbitrary linear system which is undisturbed for  $t < 0$ .) The significance of the kernel function,  $D(t-\tau, \tau)$ , is brought out by applying a constant stress at  $t = t_i > 0$ :

$$\epsilon = D(t - t_i, t_i) \sigma \quad (30)$$

where  $D = 0$  when  $t < t_i$ . Thus,  $D$  is a creep compliance that depends on the time elapsed since application of the stress,  $t - t_i$ , and the time at which the stress was applied,  $t_i$ . We see that evaluation of  $D$  requires a number of (identical) specimens, with the creep test on each one started at a different time.

## MATERIAL PROPERTY EVALUATION FOR UNIAXIAL LOADING

We shall be concerned in this section with the problem of using experimental data to determine the material properties in constitutive Eq. 8 and 10, and

to obtain a limited verification of the theory. Methods for doing this will be first outlined, and then applied to some different materials. Because of the similarity between Eq. 8 and 10, it will be sufficient to confine most of our attention to the former one.

## Equations for Two-Step Loading

When the stress is applied stepwise in time, Eq. 8 reduces to an algebraic relation that can be conveniently used to evaluate the properties. Consider, in particular, the two-step test:

$$\sigma = \begin{cases} \sigma_a, & 0 < t < t_a \\ \sigma_b, & t_a < t < t_b \end{cases} \quad (31)$$

where  $\sigma = 0$  when  $t < 0$ , and  $\sigma_a$  and  $\sigma_b$  are constants. Substitution of stress history (Eq. 31) into Eq. 8 yields for  $0 < t < t_a$ :

$$\epsilon = [g_o^a D_o + g_1^a g_2^a \Delta D \left( \frac{t}{a_\sigma^a} \right)] \sigma_a \equiv D_n^a \sigma_a \quad (32)$$

For  $t_a < t < t_b$ :

$$\epsilon = g_o^b D_o \sigma_b + g_1^b \left[ \int_{0-}^{t_a-} \Delta D(\psi - \psi') \frac{dg_2 \sigma}{d\tau} d\tau + \int_{t_a-}^t \Delta D(\psi - \psi') \frac{dg_2 \sigma}{d\tau} d\tau \right] \quad (33)$$

where  $t_a^-$  is the time immediately before the second stress  $\sigma_b$  is applied, and the superscript on a material property indicates the particular stress at which it is to be evaluated. The integrations in Eq. 33 are carried out by recognizing that  $dg_2 \sigma / d\tau$  is zero except at  $\tau = 0$  and  $\tau = t_a$ ; hence:

$$\epsilon = g_o^b D_o \sigma_b + g_1^b \left[ g_2^a \sigma_a \Delta D(\psi) + (g_2^b \sigma_b - g_2^a \sigma_a) \Delta D \left( \frac{t - t_a}{a_\sigma^b} \right) \right] \quad (34a)$$

where

$$\psi = \frac{t_a}{a_\sigma^a} + \frac{t - t_a}{a_\sigma^b} \quad (34b)$$

The next two subsections deal with the application of Eq. 32 and 34 for reducing creep and recovery data. For these cases, the use of superscripts  $a$  and  $b$  on the material properties will be dropped.

## Reduction of Creep Data

The form of the nonlinear creep compliance,  $D_n$ , shown in Eq. 32 is such that a simple graphical method can be employed to evaluate some properties and partially verify the theory. This may be seen by rewriting  $D_n$  as

$$\log(D_n - g_o D_o) = \log g_1 g_2 + \log \Delta D \left( \frac{t}{a_\sigma} \right) \quad (35)$$

where  $D_n - g_o D_o \equiv \Delta D_n$  is the transient component of the nonlinear creep compliance. Hence, if we plot

$\Delta D_n$  against  $t$  on double-logarithmic paper, curves at different stress levels can be superposed by translating them along the two axes. If the curves are shifted to the one for zero stress, the amount of horizontal ( $t$ ) shift and vertical ( $\Delta D_n$ ) shift equals, respectively,  $\log g_1 g_2$  and  $\log a_\sigma$ . The resulting so-called "master curve" is, of course, the transient component of the linear viscoelastic compliance.

It is seen, therefore, that a graphical scheme can be used to partially evaluate isothermal, nonlinear properties, and it is analogous to the familiar one employed in finding temperature-dependent properties of linear materials. Furthermore, we have a partial verification of the theory if a master curve can be formed.

Because of experimental limitations, it may not be possible to measure the true initial compliance,  $g_0 D_0$ . If this is the case, a trial-and-error procedure can be employed to estimate it as long as Eq. 35 is valid. In particular, assume different values of  $g_0 D_0$  until one is found that enables a master curve to be formed. If a considerable amount of creep occurs prior to the time at which the creep compliance can be reliably measured, this scheme may not provide the true initial compliance. However, it should be acceptable as long as the prediction of a short time response is not required for the engineering application of interest.

It is seen that creep data are not sufficient for evaluating  $g_1$  and  $g_2$  separately. Furthermore, the shifting procedure described above does not provide unique values of  $a_\sigma$  and  $g_1 g_2$  if the double-logarithmic compliance graphs are essentially straight lines; this is a very important situation because of the many materials that have the power-law representation for compliance,

$$D(\psi) = D_0 + D_1 \psi^n \quad (36)$$

Clearly, only the combination  $g_1 g_2 / a_\sigma^n$  is determined by creep data in this case.

However, we shall now show that when the stress,  $\sigma$ , is removed at  $t = t_a$ , strain data measured during the so-called recovery period,  $t > t_a$ , provide enough additional information to conveniently evaluate all properties, whether or not power law (Eq. 36) applies.

### Reduction of Recovery Data

Strain during the recovery period,  $t > t_a$ , will be denoted as  $\epsilon_r$ ; it is found from Eq. 34 by setting  $\sigma_b = 0$ :

$$\epsilon_r = \left[ \Delta D \left( \frac{t_a}{a_\sigma} + t - t_a \right) - \Delta D(t - t_a) \right] g_2 \sigma \quad (37)$$

Notice that for a linear viscoelastic material, this equation reduces to the familiar result:

$$\epsilon_r = [\Delta D(t) - \Delta D(t - t_a)] \sigma \quad (38)$$

which can be written in the equivalent form:

$$\epsilon_r = \epsilon(t) - \epsilon(t - t_a) \quad (39)$$

The significance of Eq. 39 is illustrated in Fig. 1, which shows the simple relation between creep and recovery curves when the material is linear.

While the jump in strain,  $\epsilon_0$ , at  $t = 0$  is equal to that at  $t = t_a$  for a linear material, this is not necessarily true with nonlinearity. Indeed, Eq. 32 and 37 enable us to calculate the difference in jumps, which is found to be

$$\Delta \epsilon_0 = g_2 (g_1 - 1) \Delta D(t_a / a_\sigma) \sigma \quad (40)$$

where  $\Delta \epsilon_0$  is the magnitude of the jump at  $t = t_a$  less the magnitude at  $t = 0$ . It is often true that these jumps are (approximately) equal, in which case  $g_1 = 1$ .

If it is found that the nonlinear creep and recovery data satisfy Eq. 39 over the time scale and stress range of interest, Eq. 32 and 37 are found to imply  $a_\sigma = 1$  and  $g_1 = 1$  (except for the very special case of steady-flow creep,  $\Delta D = D_s \psi$ ). We see that the simple relationship between creep and recovery illustrated in Fig. 1 reduces Eq. 8 to the modified superposition principle in (24).

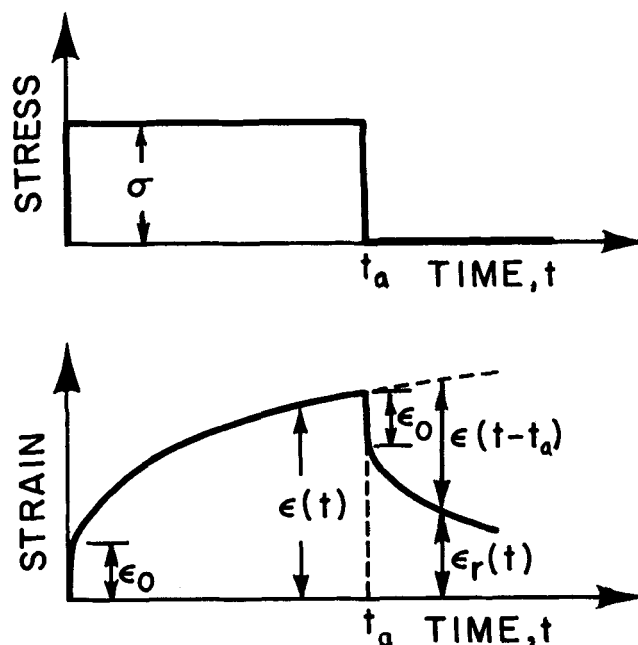


Fig. 1. Diagram of creep and recovery for a linear viscoelastic material.

For more general nonlinear behavior, Eq. 40 enables us to complete the characterization if  $g_1 g_2$ ,  $g_0$ , and  $a_\sigma$  have been found from creep data. In practice, however, the strain jump at  $t = 0$  and  $t = t_a$  may not be known accurately enough to use this equation with any degree of reliability. Nevertheless, Eq. 37 can be conveniently used to evaluate  $g_2$ , if  $a_\sigma$  is known, by matching  $\epsilon_r$  to one point on the



experimental recovery curve. Observe that it would not be necessary to know the creep compliance beyond  $t = t_a$  if the approximation

$$\Delta D \left( \frac{t_a}{a_\sigma} + t - t_a \right) \simeq \Delta D \left( \frac{t_a}{a_\sigma} \right) \quad (41)$$

can be employed at the matching point; this approximation may be quite good, even for some time beyond  $t = t_a$ , if the compliance is quite flat at the end of the creep phase.

Earlier we pointed out that creep data are not sufficient to evaluate  $g_1 g_2$  and  $a_\sigma$  when the power law (Eq. 36) exists. Eq. 41 could be matched to recovery data at more than one point to evaluate properties, but, in general, we would have to solve nonlinear algebraic equations. We shall now show that another graphical shifting procedure can be applied to recovery data, a procedure which not only avoids the solution of nonlinear equations, but also allows the "best fit" to be made by inspection.

Substitution of power law  $\Delta D = D_1 \psi^n$  into recovery strain (Eq. 37), and use of creep Eq. 32, yield

$$\frac{\epsilon_r}{\Delta \epsilon_c} = g_1^{-1} [(1 + a_\sigma \lambda)^n - (a_\sigma \lambda)^n] \quad (42a)$$

where

$$\lambda \equiv (t - t_a)/t_a \quad (42b)$$

and

$$\Delta \epsilon_c \equiv g_1 g_2 D_1 t_a^n \sigma / a_\sigma^n \quad (42c)$$

It is seen that  $\Delta \epsilon_c$  is simply the creep component of strain existing immediately before the stress is removed; viz.,  $\Delta \epsilon_c = \epsilon(t_a) - \epsilon(0)$ .

Some representative double-logarithmic plots of Eq. 42 are shown in Fig. 2 for the case  $a_\sigma = g_1 = 1$ . Now, if we were to plot experimental curves for a given material on this graph, Eq. 42 shows that a "master curve" can be formed by horizontal and vertical translations of the individual constant-stress curves. Furthermore, when this reference or master curve is for  $a_\sigma = g_1 = 1$ , the magnitude of the vertical translation is  $\log g_1$ , and that of the horizontal translation is  $\log a_\sigma$ ; if, for example, the original experimental curve lies above and to the right of the master curve, then  $a_\sigma < 1$  and  $g_1 < 1$ .

At relatively long times, the recovery curves in Fig. 2 are straight lines defined by

$$\frac{\epsilon_r}{\Delta \epsilon_c} \simeq g_1^{-1} n a_\sigma^{n-1} \lambda^{n-1} \quad (43)$$

However, up to recovery times on the order of the original creep time, there appears to be sufficient curvature to enable a unique determination of horizontal and vertical translations when forming a master curve.

### Reduction of Two-Step Strain Data

Stress response to the two-step strain input

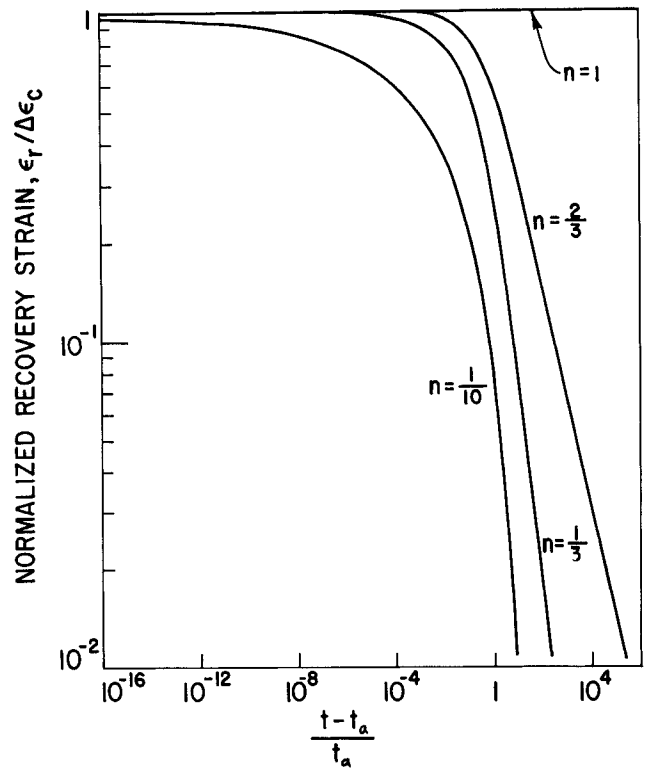


Fig. 2. Normalized recovery curves for  $D(t) = D_0 + D_1 t^n$ .

$$\epsilon = \begin{cases} \epsilon_a, & 0 < t < t_a \\ \epsilon_b, & t_a < t < t_b \end{cases} \quad (44)$$

can be conveniently used to determine material properties in Eq. 10. The data reduction method will be slightly different from that described above for creep and recovery if the tests are conducted on slender tensile specimens which necessitate  $\epsilon_b > 0$ ; assuming  $\epsilon_a$  is tensile, imposition of a zero strain,  $\epsilon_b = 0$ , would introduce a compressive stress and possibly buckling or beam-column action. Although we may not want to impose  $\epsilon_b = 0$ , it will be shown that it is desirable to make  $\epsilon_b$  as small as possible without creating a compressive stress.

By interchanging stress and strain in Eq. 32 and 34, we can write immediately the stress history due to two-step strain (Eq. 44). For  $0 < t < t_a$ :

$$\sigma = \left[ h_e^a E_e + h_1^a h_2^a \Delta E \left( \frac{t}{a_e^a} \right) \right] \epsilon_a \equiv E_n^a \epsilon_a \quad (45)$$

and, after some rearrangement, we find for  $t_a < t < t_b$ :

$$\sigma = E_n^b \epsilon_b - \left( \frac{h_1^b}{h_1^a} \right) h_1^a h_2^a \times \left[ \Delta E \left( \frac{t - t_a}{a_e^b} \right) - \Delta E \left( \frac{t_a}{a_e^a} + \frac{t - t_a}{a_e^b} \right) \right] \epsilon_a \quad (46a)$$

where

$$E_n^b \equiv h_e^b E_e + h_1^b h_2^b \Delta E \left( \frac{t - t_a}{a_e^b} \right) \quad (46b)$$

is the nonlinear relaxation modulus for a strain  $\epsilon_b$  applied at  $t = t_a$ .

Now if there is sufficient curvature in a log-log plot of relaxation data,  $E_n^a - h_e^a E_e$ , the quantities  $h_1^a h_2^a$  and  $a_e^a$  can be found by shifting the curves. Assuming single-step relaxation data are also available at strain level  $\epsilon_b$ , all quantities in the stress (Eq. 46) will be known with exception of  $h_1^b/h_1^a$ ; this ratio can then be found by matching (Eq. 46) to stress data at a convenient point in time, such as described in the previous subsection on recovery. If  $\epsilon_b$  is sufficiently small,  $h_1^b \simeq 1$ , and all properties will thereby be determined at (arbitrary) strain level  $\epsilon_a$ .

When the relaxation modulus has the common power-law form,

$$E(\rho) = E_e + E_1 \rho^{-m} \quad (47)$$

where  $E_1$  and  $m$  are constants, Eq. 46 can be written in a form analogous to Eq. 42:

$$\frac{\sigma - E_n^b \epsilon_b}{\Delta \sigma_a} = \frac{h_1^b}{h_1^a} \left[ \left( 1 + \frac{a_e^a}{a_e^b} \lambda \right)^{-m} - \left( \frac{a_e^a}{a_e^b} \lambda \right)^{-m} \right] \quad (48a)$$

where  $\lambda \equiv (t - t_a)/t_a$  and

$$\Delta \sigma_a \equiv h_1^a h_2^a \Delta E \left( \frac{t_a}{a_e^a} \right) \epsilon_a \quad (48b)$$

is the transient component of stress remaining immediately before the change in strain at  $t = t_a$ . Comparing Eq. 48 with recovery Eq. 42, we see that a graphical shifting method can be used to evaluate  $h_1^b/h_1^a$  and  $a_e^a/a_e^b$ , as discussed in the recovery subsection. Further, if  $\epsilon_b$  is sufficiently small,  $h_1^b \simeq a_e^b \simeq 1$ , and  $h_1^a$  and  $a_e^a$  can be found directly to complete the characterization for an arbitrary strain level.

When  $\epsilon_a$  is large, it may not be desirable, because of buckling, to subsequently impose a small strain  $\epsilon_b$ . However, by conducting a series of tests, starting at small strains  $\epsilon_a$  and  $\epsilon_b$ , it will be possible to use Eq. 46, or 48, together with 45, to evaluate all properties as functions of strain.

Both Eq. 46 and 48 show why the second strain,  $\epsilon_b$ , should not be close to  $\epsilon_a$ . Specifically, these equations contain property ratios which would be nearly unity if  $\epsilon_a$  and  $\epsilon_b$  were close, and experimental error might therefore mask the nonlinearity. Further, to minimize the probability of fracture, impose  $\epsilon_b < \epsilon_a$ . The same kind of conclusions apply to two-step loading discussed previously, and point up the desirability of using creep and recovery data, rather than data from two non-zero stress-steps.

### Influence of Transient Inputs

In all of our discussion on property evaluation we have assumed that the stress or strain input is changed instantaneously. In practice, of course, the time required to change the input is not zero. In-

deed, in order to avoid buckling when changing from a large to a small constant tensile strain, as discussed in the previous subsection, it may be necessary to reduce the strain over an extended period of time. Whether the finite time period is intentional or the result of experimental limitations, response data obviously will not be valid for characterization purposes until enough time has elapsed for the influence of the transient input to be negligible.

This influence has been studied analytically elsewhere (32) using linear Eq. 5 with creep compliance Eq. 36 and Eq. 7 with the familiar modified power law (15):

$$E(\rho) = E_e + \frac{E_g - E_e}{[1 + \rho/\tau_0]^m} \quad (49)$$

where  $E_g$  and  $\tau_0$  are constants; note that Eq. 49 is a generalization of Eq. 47, which accounts properly for short-time response. These viscoelastic properties, although not exactly equivalent representations of a single material, are realistic representations for polymers, and enabled analytical integration of Eq. 5 and 7 for the particular transient input employed.

A ramp input (in which stress or strain is increased at a constant rate to the time  $t_r$ , say, and is then held constant) is used in (32) to approximate the actual transient condition, and inertia effects are neglected. It is shown that response due to the ramp is within 5% of that due to a step-function input

at times  $t \gtrsim 5t_r$  for the typical range  $0 \leq m, n \leq 0.5$ , with the error being an increasing function of  $m$  and  $n$ .

### Creep and Recovery of Nitrocellulose

The remainder of this section deals with the application of the constitutive theory to isothermal behavior of three polymeric materials. The data studied are taken from the literature, rather than generated by the author, and consequently do not permit us to carry through a full critical characterization using the techniques outlined above. Nevertheless, it is hoped the examples will at least help to clarify some of the concepts and the significance of the nonlinear material properties appearing in the constitutive equations (35).

The first illustration concerns tensile creep and recovery behavior of strips of nitrocellulose film at 30°C, as reported by Van Holde (33).

The transient component of the creep compliance for this semicrystalline material was found to agree very closely with Eq. 16 except at very short times; further  $n = 1/3$  and  $g_0 \simeq 1$ .

Only two graphs of creep and recovery are shown in (33), and they have been redrawn in our Figs. 3 and 4; the open and closed circles are not necessarily original data points, but serve to define a line drawn through the data. Notice that the recovery graphs are plotted such that time is zero at the start of recovery.

As an indication of the significant amount of nonlinearity that exists, the creep amplification factor (Eq. 16b) due to nonlinearity is approximately four in Fig. 3 and three in Fig. 4.

The dashed lines indicated as Case 1 are predicted from the creep curve using Eq. 39. The agreement for the short-time creep ( $t_a = 2.8$  hr) and recovery in Fig. 3 implies that all nonlinearity is due to  $g_2$ . On the other hand, the long-time creep ( $t_a = 12$  days) and recovery do not fit this description. Since the stress and strain levels are not significantly different for the two tests, this difference in behavior may be due to aging, as hypothesized in (33).

The recovery curves indicated as Cases 2 and 3 are predictions using the original creep data, and include nonlinearity in the time-scale factor,  $a_\sigma$ ; the jumps in strain at the start of creep and the start of recovery are essentially equal for each film, which means  $g_1 = 1$ , according to Eq. 40. We were able to construct the curves for both of these cases by simply shifting horizontally the graph for Case 1 a distance equal to  $\log a_\sigma$ . This follows from recovery Eq. 42a.

All nonlinearity is in the factor,  $a_\sigma$ , for Case 2. The value of  $a_\sigma$  for Case 3 is such that the predicted and experimental recovery curves in Fig. 4 agree, except at long times.

Since creep nonlinearity, Eq. 16b, was not observed to change with time,  $g_2$  decreases with decreasing values of  $a_\sigma$ . We can think of this behavior in terms of a spring and dashpot model (13) in which the springs stiffen with age while the retardation times decrease. Further evidence that the aging hypothesis is valid is the drift to smaller values of  $a_\sigma$  at long recovery times. If the difference between behavior in Figs. 3 and 4 were due to the difference in strains, and not aging, it is believed the drift would be towards the Case 1 curve in Fig. 4 as the strain decreases in time.

### Creep and Recovery of Fiber-Reinforced Phenolic Resin

In the previous example, it was found that all nonlinearity at short times entered through the free energy-based coefficient,  $g_2$ , for the particular stress level studied. We shall now examine behavior of a reinforced amorphous polymer in which most nonlinearity is due to entropy production.

The data are reported by Martirosyan (34) from uniaxial tensile tests conducted at  $20 \pm 2^\circ\text{C}$  on phenolic resin reinforced by a 50% volume fraction of mutually perpendicular glass fibers.

The fibers were in a square array and in the plane of loading, so that the material exhibited the same properties for  $0^\circ \leq \phi \leq 45^\circ$  as for  $45^\circ \leq \phi \leq 90^\circ$ , where  $\phi$  is the angle between a fiber (principal) direction and the loading axis. Creep results (with  $t_a = 30$  minutes) are given in (34) for  $\phi = 0^\circ, 15^\circ, 30^\circ$ , and  $45^\circ$ , but recovery curves are shown for only  $\phi = 15^\circ$  and  $30^\circ$ . The material shows practically

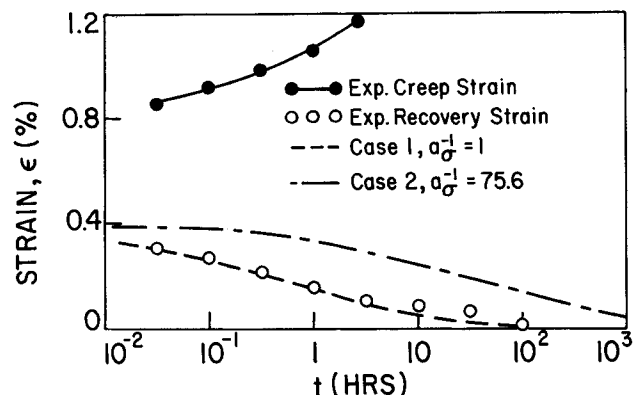


Fig. 3. Creep and recovery of nitrocellulose, film *i*,  $\sigma = 3.55$  dynes/cm<sup>2</sup> (data from Ref. 33).

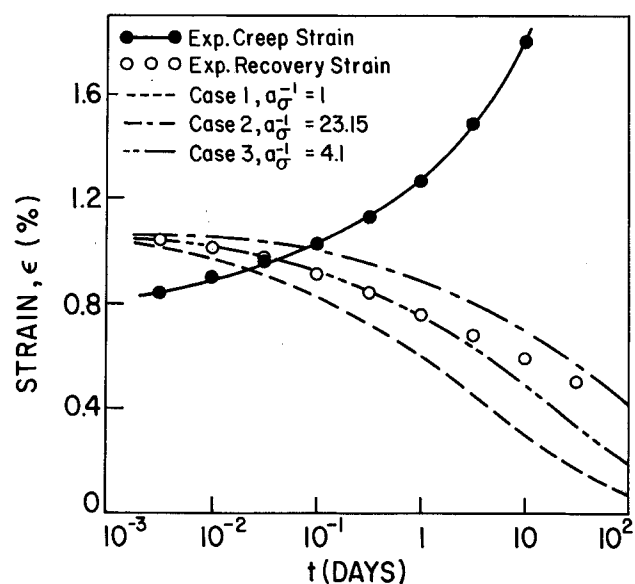


Fig. 4. Creep and recovery of nitrocellulose, film *h*,  $\sigma = 3.14$  dynes/cm<sup>2</sup> (data from Ref. 33).

negligible creep when loaded along the fibers ( $\phi = 0^\circ$ ), but is highly time dependent at the other angles. Fig. 5 shows some typical creep and recovery data; stresses are referred to initial areas, and the ultimate tensile strength reported for this angle is 1300 kgf/cm<sup>2</sup>.

The strain jumps at  $t = 0$  and  $t = t_a$  are found to be essentially equal and linear in stress, which implies  $g_0 = g_1 = 1$ . On the other hand, the time-dependent response is highly nonlinear as shown by the recovery curve (2) in Fig. 5 (which was predicted using Eq. 39) and by the stress dependence of the creep compliance in Fig. 6; the symbol  $D_\phi$  is now used for creep compliance in order to indicate the fiber angle.

So far we have found that  $g_0 = g_1 = 1$ ; of interest now is the evaluation of the remaining two nonlinear properties,  $g_2$  and  $a_\sigma$ . A graphical procedure based on Eq. 35 was given earlier for finding these

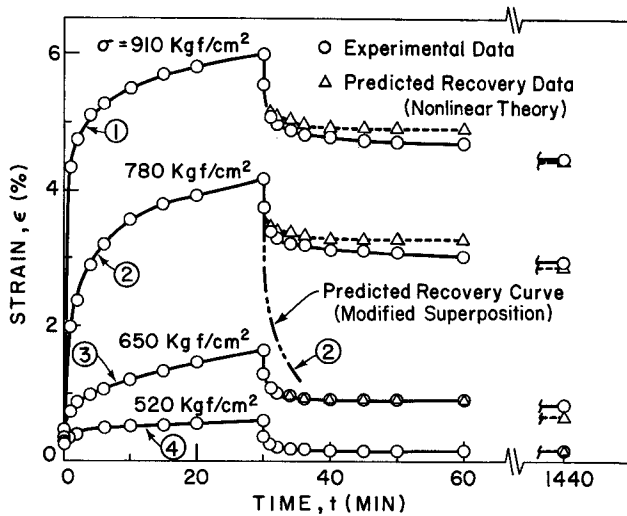


Fig. 5. Creep and recovery of glass-reinforced phenolic resin,  $\phi = 30^\circ$  (data from Ref. 34).

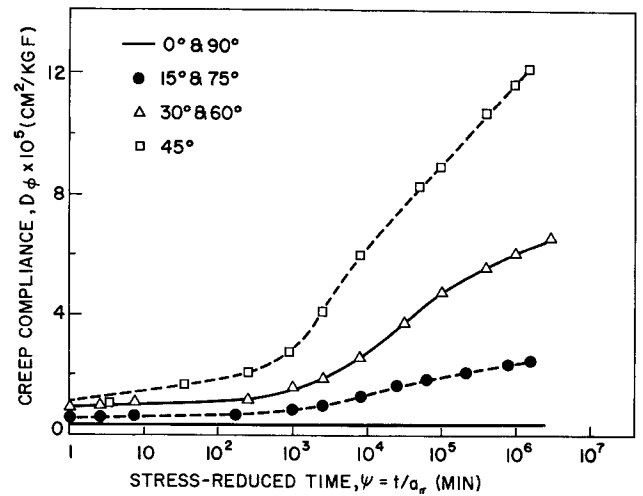


Fig. 7. Master creep compliance curves for glass-reinforced phenolic resin.

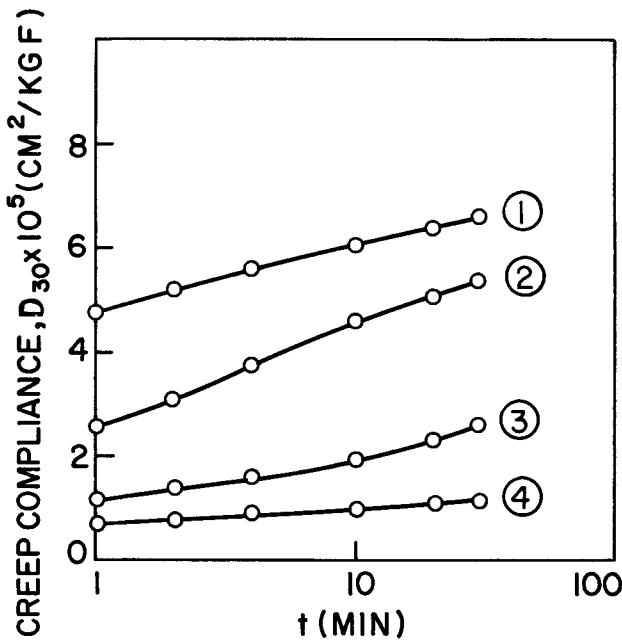


Fig. 6. Creep compliances from data in Fig. 5.

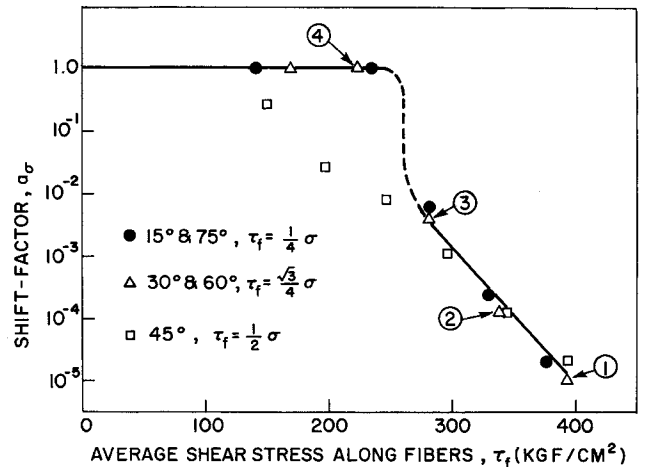


Fig. 8. Stress dependence of the horizontal shift-factor,  $a_\sigma$ . Determined by forming master curves in Fig. 7.

functions; it involved making a log-log plot of creep data and then shifting the individual constant-stress curves. Recall that the method enables both functions to be found from creep data if sufficient curvature is present in this plot, which turned out to be the case for the material under discussion. Within the ability to read values off the strain curves in (34), it was found that only a horizontal shift was needed to form the "master curve"; hence,  $g_2 = 1$ . (It should be noted that this conclusion is somewhat uncertain at low stresses because the reading error at small strain levels was magnified by the use of a logarithmic scale for compliance, and led to considerable scatter.) Now, since all nonlinearity is apparently due to  $a_\sigma$ , material properties can be determined graphically by using a linear scale for compliance. Accordingly, we obtained  $a_\sigma$  and the master

compliance curve for each fiber angle by horizontal shifting of creep data (such as illustrated in Fig. 6). The resulting master curves are drawn in Fig. 7, and in Fig. 8 the amount of horizontal shift needed is plotted against average shear stress along the fibers:

$$\tau_f = \frac{\sigma}{2} \sin 2\phi$$

It is very interesting to find that the extent of nonlinearity, as reflected by  $a_\sigma$ , depends primarily on the invariant  $\tau_f$ , and not on the average stress normal to the fibers. This may be due to the support offered by the mutually orthogonal arrangement of the relatively stiff fibers.

It is also observed that the material apparently "yields" since very little nonlinearity and creep occur

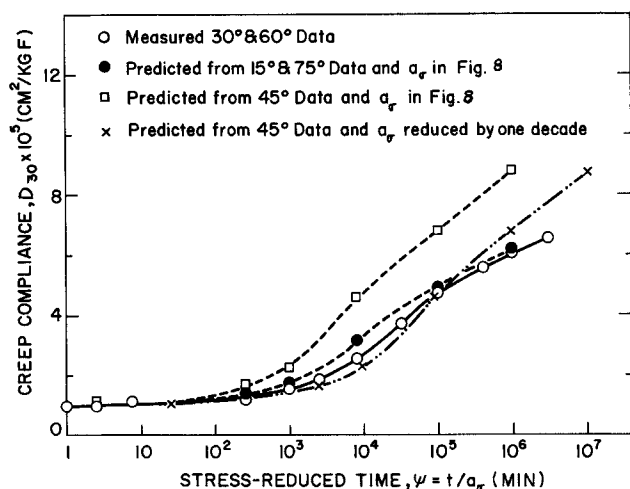


Fig. 9. Correlation of creep compliances for the different fiber orientations shown in Fig. 7.

until a critical shear stress of approximately 150 kgf/cm<sup>2</sup> is reached. This could possibly represent the start of cracking, as suggested by Halpin (30), and/or the initiation of flow of the plastic matrix. Note that at high stresses  $a_{\sigma} \sim e^{-|\gamma\tau|}$  (where  $\gamma$  is constant); this seems to indicate that the stress-dependent activation energy concept (3), based on Eyring's rate process theory, is applicable here.

We should add that there is some uncertainty in the values of  $a_{\sigma}$  at low stresses, as indicated by the dashed line in Fig. 8, because of the small slope of the short-time compliances in Fig. 7 and the inability to accurately read strain values in (34). However, we found recovery predictions were somewhat sensitive to  $a_{\sigma}$  in this range, and the low stress points shown in Fig. 8 were selected on the basis of one recovery curve for each angle reported, (i.e.,  $\phi = 15^\circ$  and  $30^\circ$ ).

The prediction of recovery using Eq. 37 with  $g_2 = 1$  was found to be very successful for both  $\phi = 15^\circ$  and  $\phi = 30^\circ$ , as illustrated in Fig. 5 for  $\phi = 30^\circ$ . It is to be noted that the effect of stress is the same as temperature in a linear thermorheologically simple material. Namely, a linear material would exhibit the same type of creep and recovery if its temperature were high during creep and low during recovery.

Another check on the theory can be made by recognizing that  $D_{\phi}$  is a fourth order tensor component, and consequently must transform in a definite manner. For the particular angles studied, the following relations must hold:

$$\begin{aligned} D_{30} &= 3 D_{15} - 2 D_0 \\ D_{30} &= 0.75 D_{45} + 0.25 D_0 \end{aligned} \quad (50)$$

where the subscript denotes the different angles represented in Fig. 7. Eq. 50 was used to predict the curves in Fig. 9. It is seen that there is good agreement if values for  $a_{\sigma}$  at  $45^\circ$  are used which are

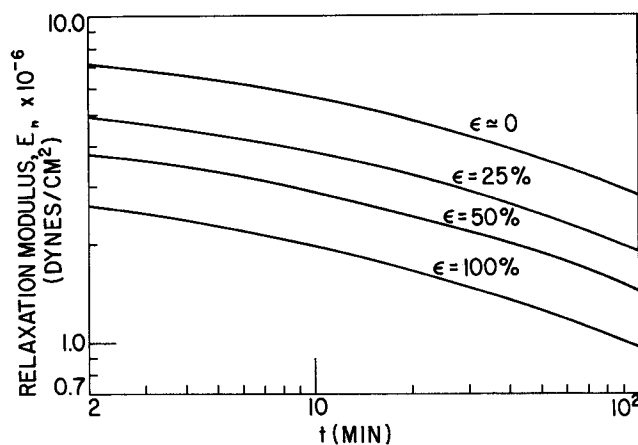


Fig. 10. Nonlinear stress relaxation modulus of PIB (data from Ref. 36).

shifted one decade downward from the data in Fig. 8\*. Since we found the original  $45^\circ$  creep curves can be represented as well by this corrected  $a_{\sigma}$  as the original one, Eq. 50 is not necessarily in error. Instead, an invariant slightly different from  $\tau_f$  may actually be needed in order to account for the stress normal to the fibers; for example, a generalization of the octahedral shear stress criterion to anisotropic materials could be tried (28, p. 228; 35).

Although the (dominant) nonlinearity for this reinforced plastic appears to enter in the shift factor,  $a_{\sigma}$ , this will not always be the case. Some of our own experimental results for multiple-step loading and unloading of unidirectional, glass fiber-reinforced epoxy are described by constitutive Eq. 8, but all nonlinear properties are functions of the average octahedral shear stress in the epoxy.

### Multiple-Step Stress Relaxation of PIB

As a final illustration of uniaxial behavior, we shall examine briefly the response of polyisobutylene (PIB) at  $25^\circ\text{C}$  to multiple-step tensile straining.

From the data given in (36) we have constructed the nonlinear relaxation curves in Fig. 10; as in all previous considerations,  $\sigma$  is force per unit initial area and  $\epsilon$  is the ratio of length increase to initial specimen length. The relaxation curves for this uncross-linked, amorphous polymer are in the long-time range close to the so-called terminal zone (1, p. 29).

The curves in Fig. 10 are such that they can be superposed quite well by means of vertical translations only; slightly better superposition is realized if a small horizontal translation ( $a_{\epsilon} \approx 0.8$  at  $\epsilon = 100\%$ ) is also used, but this has been neglected here. On this basis, the nonlinear relaxation modulus has

\* The relatively high strain rate implied by the shifted  $45^\circ$  compliance at long times is possibly due to a greater decrease in cross-sectional area accompanying the relatively large strains.

the product form (Eq. 19). Further, with a maximum error of about 5% at intermediate strains we have found

$$(1 + \epsilon) \sigma \simeq E(t) \ln(1 + \epsilon) \quad (51)$$

or, equivalently,

$$h_1 h_2 \simeq \frac{\ln(1 + \epsilon)}{\epsilon(1 + \epsilon)} \quad (52)$$

(Note that  $E_e = 0$  for an uncross-linked polymer.)

For this essentially incompressible material,  $(1 + \epsilon)\sigma$  is the true stress,  $\sigma_T$ ; i.e.,  $\sigma_T$  is stress based on the current cross-sectional area. Therefore Eq. 51 suggests that the material is approximately linearly viscoelastic in terms of true stress and natural strain; this would imply  $h_2 = \ln(1 + \epsilon)/\epsilon$  and  $h_1^{-1} = 1 + \epsilon$ . Whether or not this is indeed the correct decomposition can be determined from two-step relaxation data, based on our previous discussion.

Because of the limited amount of this data available, we have used a trial approach instead by assuming the constitutive equation

$$\sigma_T = f_1 \int_0^t E(t - \tau) \frac{d}{d\tau} \ln(1 + \epsilon) d\tau \quad (53)$$

where  $f_1 = f_1(\epsilon)$  is close to unity and accounts for the fact that the actual product  $h_1 h_2$  is not given exactly by Eq. 52. The equation has been found to accurately predict the two- and three-step data in (36), and the three-step result is shown in Fig. 11 the strain history for this case is

$$\epsilon = \begin{cases} \epsilon_a, & 0 < t < t_a \\ \epsilon_b, & t_a < t < t_b \\ \epsilon_c, & t > t_b \end{cases} \quad (54)$$

Finally, we observe that when  $f_1 = 1$ , Eq. 53 is equivalent to the so called BKZ theory used in (36), which accounts for the fact that predictions of the two theories are found to be essentially the same for this material.

## ON CONSTITUTIVE EQUATIONS FOR MULTIAXIAL LOADING

The discussion so far has demonstrated the feasibility of characterizing nonlinear viscoelastic materials, under uniaxial loading, in terms of linear viscoelastic creep and relaxation functions. Analogous constitutive equations for general multiaxial states of stress and strain are derived in (12, 13). Although the only time-dependent properties that enter are the linear viscoelastic creep and relaxation functions, further simplification is needed in order to be able to evaluate the nonlinear material functions with any kind of a practical experimental program. In this section we shall briefly discuss some behavior of metals and plastics, and use this as a guideline for proposing a simplified three-dimensional theory.

First of all, we saw that the fiber-reinforced plastic studied in the previous section behaved essen-

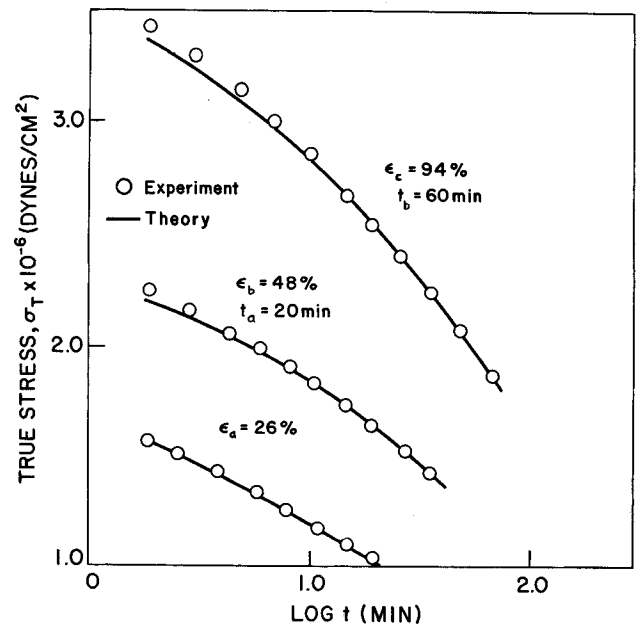


Fig. 11. Triple-step stress relaxation of PIB (data from Ref. 36).

tially as a linear viscoelastic material, but with an intrinsic time-scale that depended on average shear stress parallel to the fibers. Only uniaxial loading data were available, but such an interpretation may carry over to multiaxial loading, at least in the plane of the fibers. In such a case, uniaxial tests would be sufficient to characterize the material.

We have shown (4) that the classical engineering theories for multiaxial, inelastic behavior of metals are contained in this same description, except that the intrinsic time scale is a function of the octahedral shear stress and/or strain. Again, uniaxial tests are sufficient to evaluate material properties.

Some creep data on a tube of polyvinylchloride (PVC) under combined tension and torsion were reported by Onaran and Findley (37). Although the data are not sufficient to determine whether or not more than one nonlinear function is needed under variable loading, we would like to show that the nonlinearity under constant stress can be expressed (approximately) as a function of the octahedral shear stress.

According to (37), the tensile strain,  $\epsilon_{11}$ , due to a constant, normal stress,  $\sigma_{11}$ , acting alone, can be expressed as

$$\epsilon_{11} = (D_o + f_{11} t^n) \sigma_{11} \equiv D_n \sigma_{11} \quad (55)$$

where  $f_{11}$  is a function of  $\sigma_{11}$ , and  $D_o$  and  $n$  are constants; here,  $n = 0.155$ . Similarly, the shear strain (torsion),  $\epsilon_{12}$ , due to a constant shear stress,  $\tau_{12}$ , is

$$\epsilon_{12} = [J_o + f_{12} t^n] \tau_{12} \equiv J_n \tau_{12} \quad (56)$$

where  $f_{12}$  is a function of  $\tau_{12}$ , and  $J_o$  is a constant; note that the same exponent,  $n$ , appears in Eq. 55 and 56.

Expressions for tensile and shear strain under constant combined stresses are identical with Eq. 55 and 56, but the creep coefficients depend on both tensile and shear stress. These coefficients are given in Table IA in (37), and in Fig. 12 we have plotted them against the so-called effective stress,  $\sigma_e$ . This quantity is an invariant which is proportional to the octahedral shear stress,  $\bar{\tau}$ ; viz.,  $\sigma_e \equiv 3\tau/\sqrt{2}$ . It is used instead of  $\bar{\tau}$  for convenience, because under a uniaxial stress  $\sigma_e$  reduces to this stress. For the particular case of shear stress plus tension it becomes

$$\sigma_e = \sqrt{\sigma_{11}^2 + 3\tau_{12}^2} \quad (57)$$

We observe from Fig. 12 that this invariant accounts quite well for the combined stress effect in  $f_{11}$  and  $f_{12}$ .

It is to be noted that the combined stress data reflect a considerable amount of torsion and tension interaction, and are sufficiently sensitive to distinguish between the use of Eq. 57 and another invariant commonly used for metals; viz., maximum shear stress. The maximum shear stress is proportional to  $\sigma_e'$ :

$$\sigma_e' = \sqrt{\sigma_{11}^2 + 4\tau_{12}^2} \quad (58)$$

We found that the data plotted against  $\sigma_e'$  did not superpose nearly as well as that shown in Fig. 12.

If the yield stress is interpreted as a stress required to cause appreciable softening, such as is reflected by a rapid increase in creep coefficient,  $f_{11}$ , say, then these findings on the effective stress are consistent with yield data on polymethylmethacrylate in (3).

The simple relationship between the dashed lines in Fig. 12 is very interesting. Specifically, consider first the Poisson's ratio,  $\nu(t)$ , for a linear viscoelastic material. Under constant stress it is related to the creep compliance in tension,  $D(t)$ , and shear  $J(t)$  in the same way as for an elastic material:

$$\nu(t) = \frac{J(t)}{D(t)} - 1 \quad (59)$$

where  $D(t) = D_n$  and  $J(t) = J_n$  when the stresses are sufficiently small. We should add that  $\epsilon_{12}$  in Eq. 56 is the tensor definition of shear strain, which is one-half of "engineering" shear strain; as a result  $J$  is one-half of the more commonly used shear compliance.

Now we find that the dashed curve of shear coefficient,  $f_{12}$ , in Fig. 12 can be superposed on the tension coefficient curve,  $f_{11}$ , by a vertical translation. This implies that  $f_{12}/f_{11}$  is approximately constant, which turns out to be equal to  $J_o/D_o \approx 1.35$ . Therefore, a Poisson's ratio given by Eq. 59, but in terms of nonlinear compliances, is essentially independent of stress and time.

It is not difficult now to construct a set of small-strain, three-dimensional constitutive equations, one which includes the above behavior for PVC as a special case, which is consistent with the thermodynamic theory in (13), and which yet enables all

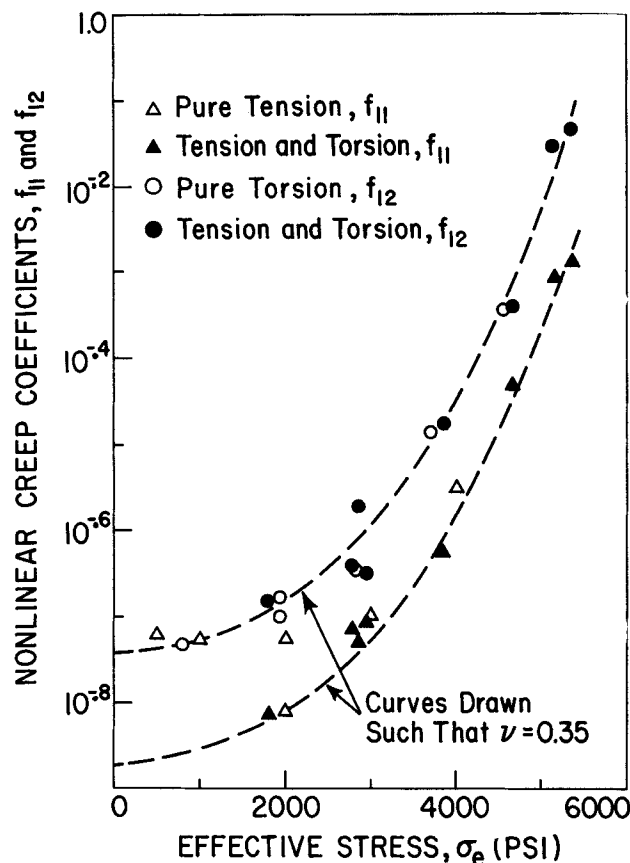


Fig. 12. Nonlinear creep coefficients for combined tension and torsion of PVC (data from Ref. 37).

properties to be evaluated from uniaxial tests.

Specifically, for initially isotropic materials with properties  $g_o = g_1 = 1$ , a suggested generalization is:

$$\epsilon_{11} = D\{\sigma_{11} + \sigma_{22} + \sigma_{33}\} - J\{\sigma_{22} + \sigma_{33}\} \quad (60)$$

and two analogous equations for  $\epsilon_{22}$  and  $\epsilon_{33}$ ; also

$$\epsilon_{12} = J\{\tau_{12}\} \quad (61)$$

and two analogous equations for  $\epsilon_{23}$  and  $\epsilon_{13}$ . The stresses and strains are referred to Cartesian coordinates  $x_i$ , and  $D\{\}$  and  $J\{\}$  are linear operators defined by Eq. 8, but with  $g_o = g_1 = 1$ . For example, this equation is written as  $\epsilon = D\{\sigma\}$ ; the linear viscoelastic shear compliance  $J(\psi)$  is used in place of  $D(\psi)$  to obtain the operator  $J\{\}$ . The same material properties,  $g_2$  and  $a_\sigma$ , appear in both operators, and are scalar functions of the single effective stress invariant,  $\sigma_e \equiv 3\tau/\sqrt{2}$ .

When  $J(\psi)/D(\psi)$  is constant, the above nonlinear constitutive equations predict a constant Poisson's ratio,  $\nu \equiv -\epsilon_{22}/\epsilon_{11} = J(\psi)/D(\psi) - 1$ , with uniaxial loading, such as found for PVC. However,  $D(\psi)$  and  $J(\psi)$  in Eq. 60 and 61 are not limited to this case or to the powerlaw form.

It can be shown that these equations are exact for linear viscoelastic behavior (i.e., when  $g_o = g_1 = g_2 = a_\sigma = 1$ ), and that they contain the classical three-dimensional theory of creep of metals (4). However, in spite of the amount of data that sup-

port these equations, they certainly should not be used for a given material without adequate experimental verification. Indeed, there are additional nonlinear properties in the thermodynamic equations in (13) which may be needed.

## CONCLUSIONS

We have attempted to show the existence of a good deal of experimental evidence on a variety of nonlinear viscoelastic materials that points toward the validity of some relatively simple constitutive equations. These equations provide direct guidelines for designing experimental programs and for reducing data so as to be able to graphically evaluate material properties and verify the theory. Admittedly, a number of assumptions and approximations have been made to arrive at the proposed equations. Nevertheless, it is believed the equations are suitable for use in an engineering stress analysis of many materials.

## ACKNOWLEDGMENTS

This work was sponsored by the Air Force Materials Laboratory, Research and Technology Division, Air Force Systems Command, United States Air Force under Contract Number F 33615-67-C-1412.

The author is grateful to the project scientist, Mr. J. C. Halpin, for helpful discussions on the behavior of polymers and to Mr. Y. C. Lou for his assistance in reducing the data on fiber-reinforced plastic.

## REFERENCES

1. J. D. Ferry, "Viscoelastic Properties of Polymers," John Wiley (1961).
2. E. Passaglia and J. R. Knox, 'Viscoelastic Behavior and Time-Temperature Relationships,' Ch. 3 in "Engineering Design for Plastics," Eric Baer, Ed., Reinhold (1964).
3. R. L. Thorkildsen, 'Mechanical Behavior,' Ch. 5 in "Engineering Design for Plastics," Eric Baer, Ed., Reinhold (1964).
4. R. A. Schapery, "On a Thermodynamic Constitutive Theory and Its Application to Various Nonlinear Materials," Proc. IUTAM Symp. on Thermoelasticity, Springer-Verlag (1969).
5. C. Truesdell and W. Noll, Nonlinear Field Theories of Mechanics, "Hand. der Phys.," Springer (1965).
6. A. E. Green and R. S. Rivlin, *Arch. Rat. Mech. Anal.*, **1**, 1 (1957).
7. A. E. Green, R. S. Rivlin, and A. J. M. Spencer, *Arch. Rat. Mech. Anal.*, **3**, 82 (1959).
8. H. Leaderman, F. McCracken, and O. Nakada, *Trans. Soc. Rheol.*, **7**, 111 (1963).
9. I. M. Ward and E. T. Onat, *J. Mech. Phys. Solids*, **11**, 217 (1963).
10. V. V. Neis and J. L. Sackman, *Trans. Soc. Rheol.*, **11**, 307 (1967).
11. W. N. Findley and K. Onaran, *Trans. Soc. Rheol.*, **12**, 217 (1968).
12. R. A. Schapery, "A Theory of Nonlinear Thermoviscoelasticity Based on Irreversible Thermodynamics," *Proc. 5th U. S. Nat. Cong. Appl. Mech.*, ASME, 511 (1966).
13. R. A. Schapery, "Further Development of a Thermodynamic Constitutive Theory: Stress Formulation," Purdue University, Rept. No. 69-2 (February 1969).
14. H. Leaderman, "Elastic and Creep Properties of Filamentous Materials and Other High Polymers," The Textile Foundation, Washington, D. C. (1943).
15. M. L. Williams, *AIAA J.*, **2**, 785 (1964).
16. J. K. Mitchell, R. G. Campanella, and A. Singh, *Proc. ASCE, Soil Mech. and Foundations Div.*, **94**, 231 (1968).
17. W. N. Findley and D. B. Peterson, *Proc. Am. Soc. Testing Mater.*, **58**, 841 (1958).
18. E. Passaglia and H. P. Koppehele, *J. Polymer Sci.*, **33**, 281 (1958).
19. R. Meredith, "The Mechanical Properties of Textile Fibers," Interscience (1956).
20. A. J. Staverman and F. Schwarzl, "Die Physik Der Hochpolymeren," IV, H. A. Stuart, Ed., Springer-Verlag, (1956).
21. J. C. Halpin, *J. Appl. Phys.*, **36**, 2975 (1965).
22. J. T. Bergen, D. C. Messersmith, and R. S. Rivlin, *J. Appl. Polymer Sci.*, **3**, 153 (1960).
23. R. A. Schapery, "Approximate Methods for Thermo-viscoelastic Characterization and Analysis of Nonlinear Solid Rocket Grains," AIAA Paper No. 68-520, to appear in *AIAA J.* (1969).
24. W. N. Findley and J.S.Y. Lai, *Trans. Soc. Rheol.*, **11**, 361 (1967).
25. W. N. Findley and G. Khosla, *J. Appl. Phys.*, **26**, 821 (1955).
26. A. C. Pipkin and T. G. Rogers, *J. Mech. Phys. Solids*, **16**, 59 (1968).
27. T. L. Smith, *Polymer Eng. Sci.*, **5**, 270 (1965).
28. I. Finnie and W. R. Heller, "Creep of Engineering Materials," McGraw-Hill (1959).
29. K. Nagamatsu, T. Takemura, T. Yoshitomi and T. Take-moto, *J. Polymer Sci.*, **33**, 515 (1958).
30. J. C. Halpin, "Introduction to Viscoelasticity," in Composite Materials Workshop, S. W. Tsai, J. C. Halpin, and N. J. Pagano, Eds., Technomic (1968).
31. J. D. Ferry and R. A. Stratton, *Kolloid Z.*, **171**, 107 (1960).
32. Y. C. Lou and R. A. Schapery, "Viscoelastic Behavior of Fiber-Reinforced Composite Materials," Air Force Materials Laboratory, Tech. Rept. No. AFML-TR-68-90 (April 1968).
33. K. Van Holde, *J. Polymer Sci.*, **24**, 417 (1957).
34. M. M. Martirosyan, *Mekhanika Polimerov*, **1**, 47 (1965).
35. Y. C. Lou and R. A. Schapery, "Viscoelastic Characterization of a Nonlinear, Fiber-Reinforced Plastic, to appear in *J. Comp. Mat.* (1969).
36. L. J. Zapas and T. Craft, *J. Res. N.B.S.*, **69A**, 541 (1965).
37. K. Onaran and W. N. Findley, *Trans. Soc. Rheol.*, **9**, 299 (1965).